Advances in Radiation Oncology (2016) 1, 106-114

advances
in radiation oncology

www.advancesradonc.org

Scientific Article

Detection of late radiation damage on left atrial fibrosis using cardiac late gadolinium enhancement magnetic resonance imaging

Y. Jessica Huang PhD [a,*], Alexis Harrison MD [b,c], Vikren Sarkar PhD [a], Prema Rassiah-Szegedi PhD [a], Hui Zhao PhD [a], Martin Szegedi PhD [a], Long Huang PhD [a], Brent Wilson MD, PhD [b,c], David K. Gaffney MD, PhD [a], Bill J. Salter PhD [a]

[a] *Department of Radiation Oncology, University of Utah, Salt Lake City, Utah*
[b] *Cardiovascular Center, University of Utah, Salt Lake City, Utah*
[c] *Comprehensive Arrhythmia Research and Management Center, University of Utah, Salt Lake City, Utah*

Received 7 January 2016; received in revised form 15 April 2016; accepted 19 April 2016

Abstract

Purpose: This is a proof-of-principle study investigating the feasibility of using late gadolinium enhancement magnetic resonance imaging (LGE-MRI) to detect left atrium (LA) radiation damage.

Methods and materials: LGE-MRI data were acquired for 7 patients with previous external beam radiation therapy (EBRT) histories. The enhancement in LA scar was delineated and fused to the computed tomography images used in dose calculation for radiation therapy. Dosimetric and normal tissue complication probability analyses were performed to investigate the relationship between LA scar enhancement and radiation doses.

Results: The average LA scar volume for the subjects was 2.5 cm^3 (range, 1.2-4.1 cm^3; median, 2.6 cm^3). The overall average of the mean dose to the LA scar was 25.9 Gy (range, 5.8-49.2 Gy). Linear relationships were found between the amount of radiation dose (mean dose) ($R^2 = 0.8514$, $P = .03$) to the LA scar-enhanced volume. The ratio of the cardiac tissue change (LA scar/LA wall) also demonstrated a linear relationship with the level of radiation received by the cardiac tissue ($R^2 = 0.9787$, $P < .01$). Last, the normal tissue complication probability analysis suggested a dose response function to the LA scar enhancement.

Conclusions: With LGE-MRI and 3-dimensional dose mapping on the treatment planning system, it is possible to define subclinical cardiac damage and distinguish intrinsic cardiac tissue change from radiation induced cardiac tissue damage. Imaging myocardial injury secondary to EBRT using MRI may be a useful modality to follow cardiac toxicity from EBRT and help identify individuals who are more susceptible to EBRT damage. LGE-MRI may provide essential

Conflicts of interest: None.

* Corresponding author. Department of Radiation Oncology, University of Utah, 1950 Circle of Hope, Rm 1570, Salt Lake City, UT 84112
E-mail address: y.jessica.huang@hci.utah.edu (Y.J. Huang)

http://dx.doi.org/10.1016/j.adro.2016.04.002

information to identify early screening strategy for affected cancer survivors after EBRT treatment.

Introduction

Radiation-induced heart damage from treatment of left breast cancer,[1,2] esophagus,[3-5] and lymphoma[6-12] have been reported for decades. Some of the common late effects of cardiac toxicity include pericarditis, coronary artery disease, or myocardial infarction.[13] With the improvement of treatment techniques, 3-dimensional (3D) imaging and planning systems, advancement in treatment technologies (eg, intensity modulated radiation therapy), and implementation of active breathing control during radiation treatment, radiation dose delivered to the heart has been significantly reduced in recent years. In spite of these advances, in many clinical scenarios the heart still receives a significant dose from radiation treatment of common cancers such as lung, esophagus, breast, and lymphoma.

The consensus constraint dose to the heart for different treatment sites is still not precisely determined. Different institutions and clinical trials often use varying heart dose limitations in radiation treatment delivery. One of the biggest challenges of defining radiation induced cardiac injury relative to radiation dose is the difficulty in delineating the clinically relevant subregions of the heart from planning computed tomography (CT) images. To study the radiation dose effect to the heart, many studies have contoured the entire heart, pericardium, or the left ventricle alone as the volumes of interest for consideration.[3,5,14,15] Various imaging modalities can be used in investigating radiation-induced heart disease (RIHD).[16] Echocardiography is useful in understanding the size and shape of the heart, pumping performance and valvular disease severity evaluation. Nuclear cardiology can provide valuable information to assess blood flow, the pumping function of the heart, and the size of the heart, which enable the assessment of the disease extent and the prediction of outcomes. However, both echocardiography and nuclear cardiology do not offer detail anatomical information. Cardiac CT offers anatomical information on the heart and its vicinity; CT angiogram provides further detail pictures of the blood vessels that go to the heart. One of the main concerns about CT is the radiation exposure; it is also difficult to define clinical relevant subregions of the heart. We had chosen cardiac magnetic resonance imaging (MRI) because it is widely recognized as one of the most useful, noninvasive imaging modalities for cardiac structures, including assessment of cardiac volumes, systolic function, and evaluation of tissue structural remodeling (referred to as fibrosis).[16] Specifically, late gadolinium enhancement (LGE)-MRI is a unique imaging protocol that can be used to identify infarcted myocardial tissue and provide fibrosis assessment. Myocardial fibroses had been found to be one of the most common histologic features of the failing heart and a major independent predictive factor of adverse cardiac outcome from previous studies.[17] In the LGE-MRI, infarcted or fibrotic tissue appears with bright contrast, and studies have shown links between the amount of LGE in the myocardial tissue and prognosis in patients with cardiomyopathy.[18-22] Fallah-Rad et al[23] established the utility of LGE-MRI to identify myocardial changes (focal LGE in the left ventricle) in a group of breast cancer patients who experienced trastuzumab-induced cardiomyopathy. We believe that LGE-MRI can also offer important information for patient with external beam radiation therapy (EBRT) history. To date, the relationship between the dose from thoracic EBRT and the extent of LGE presentation has not been described.

In this study, we explore the potential of LGE-MRI to detect EBRT-induced injury to the left atrium. We hypothesize that LGE-MRI can detect the amount of fibrosis (myocardial tissue injury) in patients with previous EBRT history, and that a dose-response relationship between EBRT dose and EBRT-induced tissue injury can be defined.

Methods and materials

Patients

Seven patients with previous thoracic EBRT history (6 with lymphoma, 1 with an esophageal diagnosis), with 3.1 ± 1.9 elapsed years between EBRT and LGE-MRI acquisition were studied. The demographic information and radiation treatment history of the study subjects are presented in Table 1. All 6 of the lymphoma patients had exposure to anthracyclines. Two lymphoma patients had Hodgkin's lymphoma: 1 was treated with Stanford V and the other had early-stage disease and was treated with 2 cycles of Adriamycin-bleomycin-vinblastine sulfate-dacarbazine. Four lymphoma patients had diffuse large B-cell lymphoma and all had 6 cycles of rituximab-cyclosphosphamide-hydroxyldaunorubin-oncovin-prednisone. No patient had a previous heart condition. One patient had esophagus cancer and did not have exposure to anthracyclines. He was treated on a Radiation Therapy Oncology Group protocol and received chemoradiation

Table 1 Patient characteristics

Patient no.	Age (at time of RT/MRI)	Lapsed time (y)[a]	Treatment site, technique	Prescribed dose (Gy)	Treatment fractionation	Chemotherapy regimen
1	33/33	0.2	Left neck and mediastinum, AP/PA	20.0	10	ABVD ×2
2	31/35	4.4	Mediastinum, AP/PA	30.6	17	R-CHOP ×6
3	55/59	3.2	Right heart, 3D-CRT with oblique fields	30.6	17	R-CHOP ×6 with IT methotrexate
4	26/29	3.6	Mediastinum, AP/PA	36.0	20	Stanford V, ICE, BEAM
5	41/48	6.6	Mediastinum, LAO/RPO	36.0	20	R-CHOP ×6
6	58/61	2.4	Modified mantle, AP/PA	36.0	20	R-CHOP ×6 with IT methotrexate
7	72/74	1.5	Esophagus, 4-field box	54.3	28	Cisplatin, paclitaxel, and cetuximab
Average	45/48	3.1	-	34.8	18.9	

ABVD, Adriamycin-bleomycin-vinblastine sulfate-dacarbazine; AP, anteroposterior; BEAM, BCNU, etoposide, cytarabine, and melphalan; 3D-CRT, 3-dimensional conformal radiation therapy; ICE, ifosfamide, carboplatin, etoposide; LAO, left anterior oblique; MRI, magnetic resonance imaging; PA, posteroanterior; R-CHOP, rituximab-cyclosphosphamide-hydroxyldaunorubin-oncovin-prednisone; RPO, right posterior oblique; RT, radiation therapy.

[a] Lapsed time was the time between RT computed tomography simulation and late gadolinium enhancement-MRI dates.

to a dose of 54.32 Gy. All patients were recruited from our institution, and the study protocol was reviewed and approved by the Institutional Review Board and was Health Insurance Portability and Accountability Act–compliant.

MRI acquisition and cardiac analysis

LGE-MRI data were acquired on a Siemens Verio 3-Tesla MRI scanner (Siemens Medical Systems, Erlangen, Germany). The LGE imaging was acquired using a respiration- and electrocardiogram-gated gradient echo pulse sequence. Detailed parameters for LGE images have been previously published.[24,25] Depending on heart rate and respiratory pattern, overall scanned time for the LGE-MRI study was 4-8 minutes.

The analysis of the 3D LGE images was performed using our custom software, Corview44 (MARREK Inc., Salt Lake City, UT), a cardiac MRI analysis interface. Left and right atrial endocardial borders were manually contoured to delineate the left and right atrial walls on the 3D LGE-MRI. The contouring was performed to confine the region of interest to the wall alone, thereby avoiding the blood pool. Wall segmentation was defined as the endocardial segmentation subtracted from the epicardial segmentation. To delineate enhancement in atrial walls, a relative intensity threshold was established by an imaging expert who was blinded to the dose distribution information (eg, pixel intensity more than 3 standard deviations above the intensity found in the normal tissue). The defined enhanced areas were then verified independently to ensure the appropriateness of lesion detection. A detailed description of atrial wall enhancement delineation can be found in the published manuscript.[24]

Image registration and dose mapping

All EBRT treatment plans used for previous radiation treatment of the patient were developed in the Eclipse 10.0 (Varian Medical System, Palo Alto, CA) treatment planning system (TPS). We imported 3D LGE-MRI with delineated atrial walls and scars of these patients into the Eclipse TPS. 3D CT images with 1 second rotation time were acquired at the time of simulation and were registered with the delineated 3D LGE-MRI (rigid registration). The 3D/3D rigid registrations were performed by the same medical physicist for all data sets and verified by a second medical physicist. The registration process used auto-matching with Mutual Information,[26,27] with region of interest areas specified at the heart, followed by manual match (translate/rotate) to fine tune the final registration. Figure 1 shows a representative image set and the registered result with the atrial wall designated as the region of interest, along with MRI-delineated structures.

Once images were registered, 2 structures were defined, LA scar and LA wall, based on the LA scar and LA wall delineations shown on the 3D LGE images. In 6 of the patients we studied, we also delineated right atrium (RA) scar and RA wall to investigate whether a relationship can be found between RA scar volume and radiation doses. One patient did not have RA structure delineation and therefore was excluded from this part of the study. After identifying LA/RA scar and LA/RA wall,

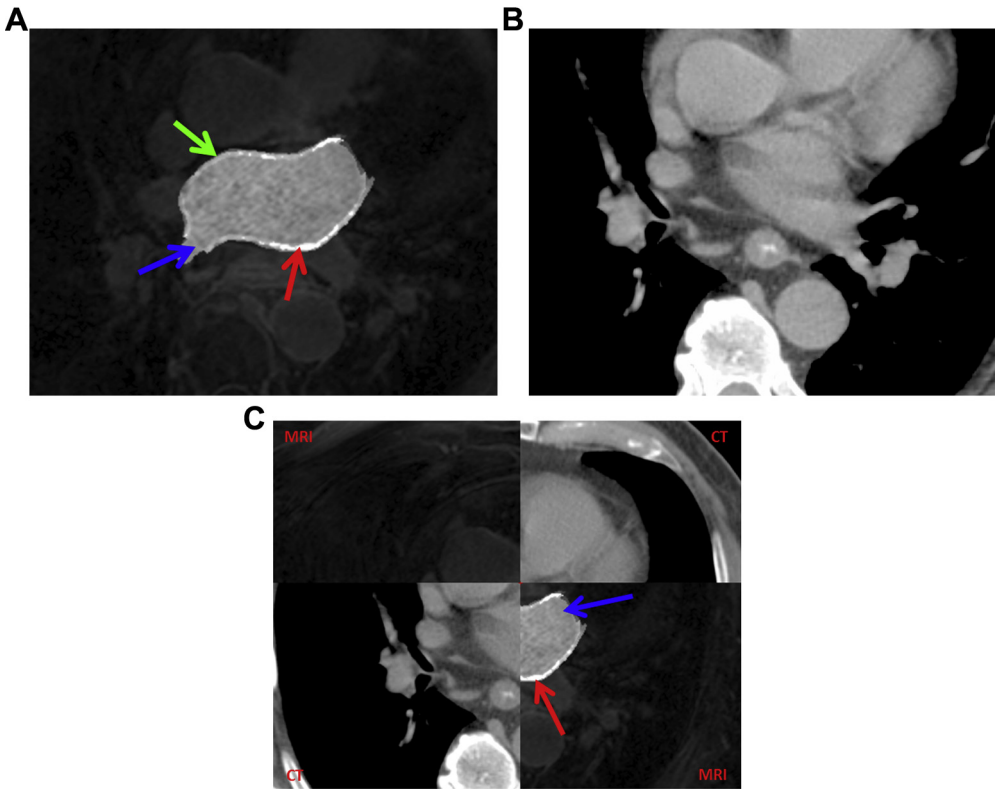

Figure 1 (A) Late gadolinium enhancement magnetic resonance imaging (LGE-MRI) with masked structures. Red arrow, left atrium (LA) scar (white structure); green arrow, LA wall (light gray structure); blue arrow, LA blood pool (darker gray). (B) Computed tomography scan taken at the time of simulation for treatment planning showing the same region of interests as the LGE MRI. (C) Rigid computed tomography/MRI registration results with split window view. Red arrow, LA scar; blue arrow, LA blood pool.

radiation doses to these structures were recorded based on dose-volume histogram (DVH) data from the TPS.

Dosimetric analysis

Doses received by both structures were visualized on multiple transverse viewing planes (Fig 2), and quantified by DVH. The dose parameters obtained from the DVH analysis included minimum dose (Dmin), maximum dose (Dmax), and mean dose (Dmean). We studied the relationship between the dose received by the LA scar and the amount of LA scar in 2 ways: first, by observing the relationship between Dmean versus LA scar volume, and, second, by characterizing and record the LA scar/LA wall ratio versus dose magnitude. This was done by obtaining the amount of LA wall and LA scar volume that were irradiated by different dose levels (<5 Gy, 5-<10 Gy, 10-<15 Gy, 15-<20 Gy, and >20 Gy), and the percentage of the LA scar/LA wall were recorded according to their dose levels from all patients (Fig 3). Additionally, all radiation doses were also converted to equivalent dose delivered in 2-Gy per fraction (EQD2) for comparison purposes. Because RIHD is considered a late effect, typical choices of alpha/beta ratio range between 2 and 3.[3,14,28,29] We therefore chose to use an alpha/beta ratio of 2.5 for calculation of bio-doses EQD2.

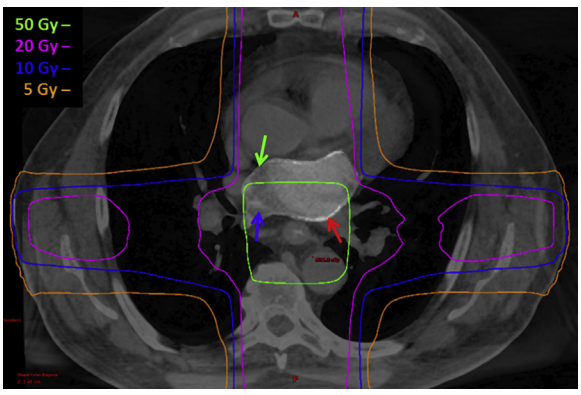

Figure 2 Treatment plan showing isodose distribution for treatment of the esophagus using 3-dimensional conformal four field technique overlaid on blended computed tomography/magnetic resonance imaging. Red arrow, left atrium scar; blue arrow, left atrium blood pool; green arrow, left atrium wall.

Normal tissue complication probability analysis

Normal tissue complication probability (NTCP) is defined as the probability of a defined complication occurring in patients because of radiation treatment. For our purposes, it was defined as the generation of scar

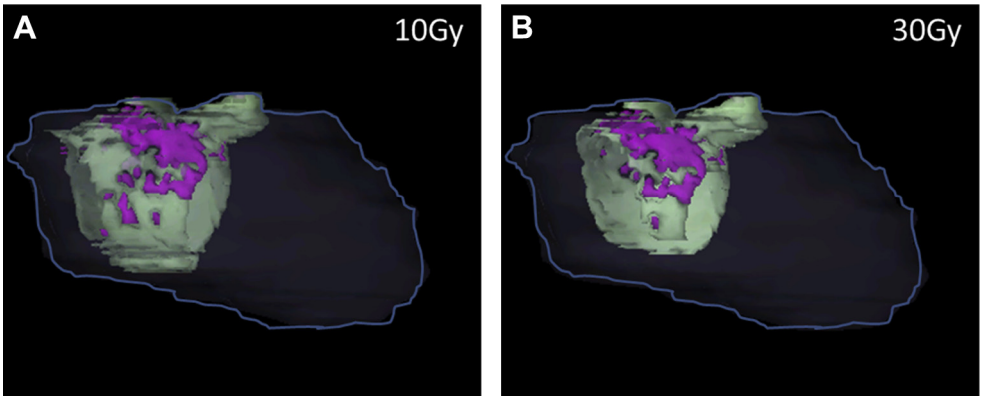

Figure 3 Left atrium (LA) wall and LA scar 3-dimensional display in different dose levels to demonstrate higher dose level resulted in higher percentage of LA scar/LA wall ratio for 1 of the cases. The heart is shown in dark gray line; LA wall in light green; LA scar in magenta. (A) The amount of LA wall and LA scar that were irradiated with 10 Gy; LA scar/LA wall: 17.3%. (B) The amount of LA wall and LA scar that were irradiated with 30 Gy; LA scar/LA wall: 22.0%.

tissue in the LA wall. Details of the methodology we used for calculating NTCP have been previously published.[30-32] Briefly, NTCP for all patients were calculated based on the DVH plot to LA scar volume. The calculation of NTCP was performed using the CERR toolkit.[33] Parameters used for the evaluation were TD50 = 70.3 Gy, r = 0.96, and s = 1, according to Eriksson.[28] We then evaluated the relationship between NTCP and our studied complication, LA scar, to determine if a correlation existed.

Statistical analysis

All statistical tests were conducted using Microsoft Office Excel 2010 (Redmond, WA). We used regression analysis in this study to observe the relationship between different parameters. Any resulting R square >0.8 was considered to be in a linear relationship.

Results

We did not observe any focal left or right ventricle myocardial injury; we also noted a more significant enhancement in the LA that was absent in the RA. No relationship can be established between RA scar and radiation dosage.

Depending on the treatment site, the radiation therapy prescribed dose to the 7 patients we studied ranged between 20 and 54.3 Gy, with an average of 34.8 Gy, in 10-28 fractions. The dosimetric parameters we collected, by patient, are listed in Table 2. The average LA scar volume for all subjects was 2.5 cm^3 (range, 1.2-4.1 cm^3; median, 2.6 cm^3); the average RA scar volume for 6 patients was 0.76 cm^3 (range, 0-2.9 cm^3; median, 0.3 cm^3). The average of Dmean to the LA scar was 25.9 Gy (range, 5.8-49.2 Gy) and for RA scar was 18.8 Gy (range, 1.1-35.7 Gy). Three of the cases (patients 1, 4, and 5) had zero RA scar volume, and the largest RA scar volume was not originated from the highest Dmean value. Because no obvious pattern was found in the relationship between RA scar volume and Dmean, no further dosimetric evaluation was performed for RA scar. The results for bio doses (EQD2) for minimum, maximum, and mean doses to LA scar, and NTCP are given in Table 3. No correlation was found between the age of the patient, either at time of RT (R^2 = 0.423, P = .114) or at time of MRI (R^2 = 0.408, P = .123), and the LA scar amount. There was also no

Table 2 Dosimetric Results for LA scar and RA scar

Patient no.	Scar (cm^3)	Dmin (Gy)	Dmax (Gy)	Dmean (Gy)
LA scar				
1	1.2	0.51	16.21	5.80
2	1.3	4.13	25.04	19.83
3	1.4	1.02	30.30	6.28
4	2.6	5.11	37.29	32.03
5	3.1	7.97	39.27	35.83
6	3.6	3.67	36.92	32.09
7	4.1	5.97	58.84	49.25
Average	2.5	4.05	34.84	25.87
RA scar[a]				
1	2.9	0.28	18.40	10.76
2	0	2.30	32.50	17.79
3	0.6	4.37	32.53	17.04
4	0	5.11	37.29	32.03
5	0	21.34	21.92	21.65
6	1.1	2.65	33.53	19.60
Average	0.76	11.06	29.16	18.81

Dmax, maximum dose; Dmean, mean dose; Dmin, minimum dose; LA, left atrium; RA, fight atrium.

[a] Only the initial 6 patients received analysis on RA scar. Because our early results from RA did not demonstrate an obvious trend with radiation doses, we excluded further RA analysis for patient number 7.

Table 3 EQD2 and NTCP results

Patient no.	LA scar (cm^3)	EQD2-Dmin (Gy)	EQD2-Dmax (Gy)	EQD2-Dmean (Gy)	EUD (Gy)	NTCP, %
1	1.2	0.29	14.84	3.97	5.64	16.91
2	1.3	2.51	22.11	16.16	19.52	22.63
3	1.4	0.58	28.83	4.00	5.89	17.01
4	2.6	3.13	36.17	29.20	26.16	25.71
5	3.1	5.13	38.95	34.17	36.57	30.94
6	3.6	2.19	35.66	29.27	32.17	29.67
7	4.1	3.60	60.16	46.61	50.89	38.80

Dmax, maximum dose; Dmean, mean dose; Dmin, minimum dose; LA, left atrium; RA, fight atrium.

correlation between the lapsed time and the amount of LA scar volume ($R^2 = 0.004$, $P = .894$).

The scatter plot of Dmean versus LA scar volume (Fig 4A) and EQD2-Dmean versus LA scar volume (Fig 5) both showed linear relationships ($R^2 = 0.851$ and 0.864, $P = .003$ and .002, respectively). Figure 4B was a scatter plot of Dmean versus RA scar volume, in which no obvious relationship was found. The linear relationship in Figs 4A and 5 suggested that increasing Dmean or EQD2-Dmean results in a higher volume of cardiac tissue changes as defined by 3D LGE-MRI. When looking at the change in ratio of LA scar/LA wall as a function of 5 dose level groups, <5 Gy, 5-10 Gy, 10-15 Gy, 15-20 Gy, and >20 Gy, a linear relationship was found between the dose level and the ratio of LA scar/LA wall (Fig 6) ($R^2 = 0.9787$, $P < .01$). NTCP results are listed in Table 3 and plotted against the scar volume (Fig 7). The

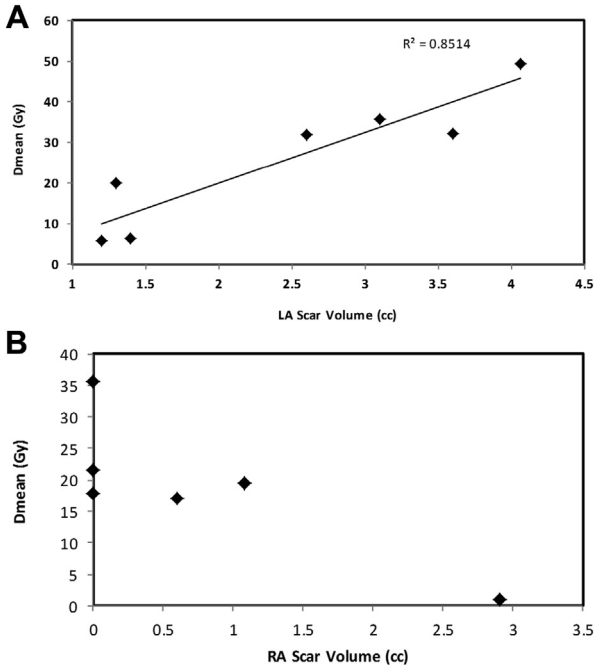

Figure 4 Scatter plot of (A) Dmean versus left atrium (LA) scar volume. (B) Dmean versus right atrium (RA) scar volume.

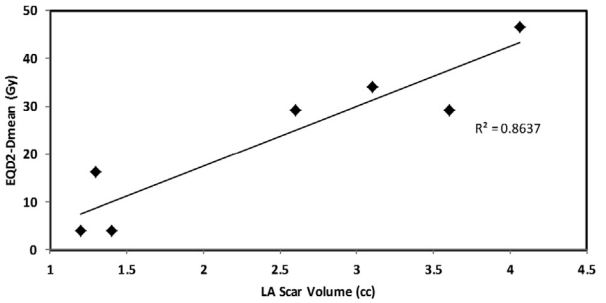

Figure 5 Scatter plot of equivalent dose delivered in 2-Gy per fraction (EQD2)-mean dose (Dmean) versus left atrium (LA) scar volume.

relationship between NTCP and LA scar volume was also shown to be relatively linear ($R^2 = 0.883$, $P < .01$), suggesting a dose response function.

Discussion

We evaluated the use of LGE-MRI to detect EBRT-induced injury in cardiac tissue and found a significantly greater degree of LGE-MRI–indicated myocardial injury in radiation areas treated with higher doses ($P < .01$). In this study, we found a significant relationship between LA scar appearance in LGE-MRI versus patients with EBRT history, regardless of the elapsed time between EBRT and LGE-MRI acquisition. Other cardiac risk factors, such as gender, race, and smoking history were not taken into consideration relative to the amount of cardiac tissue injury. Previous studies of RIHD have shown that the incidence of heart damage varies with the dose, fractionation, and irradiated volume of the heart.[1,34-37] Many of these studies typically used symptomatic cardiac disease as the study end point. However, to be able to accurately describe the risk of long-term radiation-induced heart injury for patients who previously underwent EBRT, it is important to have an early response indicator of damage. To our knowledge, this is the first study to link LGE-MRI delineated myocardial changes to EBRT cardiac doses. In this pilot study, we were able to show in 7 patients a near linear dose response between Dmean and LA scar volume ($R^2 = 0.8514$, $P = .03$). Our results correlate well with Darby et al's recent study, which used symptomatic cardiac disease as the evaluation parameter.[29] Darby looked into patients with invasive breast cancer with EBRT history who experienced major coronary events (ie, diagnosis of myocardial infraction, coronary revascularization, or death from ischemic heart disease) to analyze the effect of RIHD. Darby's result showed a linear increasing risk of major coronary event with radiation exposure. Other previous studies have also documented increasing cardiovascular disease with increasing EBRT doses.[16]

To evaluate patients for cardiac late effects post-EBRT, various screening and diagnostic tests have been

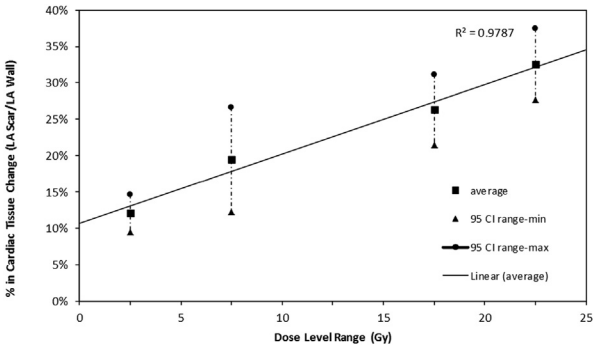

Figure 6 Relationship between dose level and the percentage of cardiac tissue change (left atrium [LA] scar/LA wall). The data shown were in 5 dose level groups: ≤5 Gy, 5-10 Gy, 10-15 Gy, 15-20 Gy, and ≥20 Gy. The resulting average cardiac tissue changes were 12.06% (95 confidence interval [CI], 9.45-14.67%), 19.48% (95 CI, 12.27-26.67%), no data available for dose level of 10-15 Gy, 26.33% (95 CI, 21.48-31.18%), and 32.56% (95 CI, 27.73-37.39%), respectively.

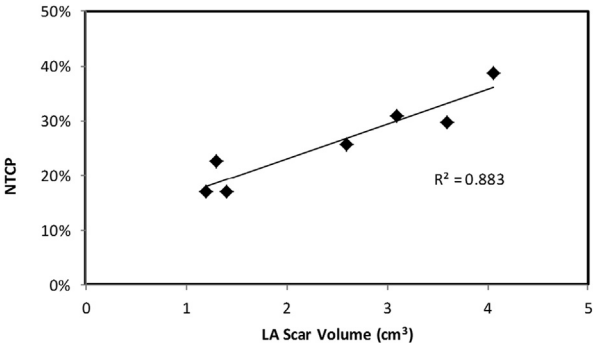

Figure 7 Scatter plot of normal tissue complication probability (NTCP) result versus left atrium (LA) scar volume.

used, such as electrocardiogram, chest radiograph, lipid profile, exercise stress test, cardiac MRI, cardiac CT, and echocardiogram.[16,38] The general consensus dose of concern identified in these studies was a heart dose of more than 30 Gy (without chemotherapy) or with fractionated dose of more than 2 Gy.[16,39,40] Furthermore, Darby et al looked into risk of ischemic heart disease after breast radiation therapy and concluded that was an increasing magnitude of the risk of 7.4% per Gray with no apparent threshold below which there was no risk. Many of the previous studies evaluated RIHD using different imaging modalities to detect functional abnormalities, without correlation of the actual radiation treatment volume.[41-45] Our results also show the same trend of higher radiation damage with increasing dose. LGE-MRI with registered radiation dose map may provide more information in future detection of RIHD at even lower doses. Furthermore, it may be able to distinguish intrinsic subclinical damage to the LA wall from actual radiation damage, as shown in Fig 6, where approximately 11% of cardiac tissue change was found when extrapolating dose level to 0 Gy. More data will need to be collected to confirm this hypothesis. With guidelines for cardiac effect after RT still being inconclusive, subclinical findings such as this one will help distinguish those who need close follow up post-RT from those who may be at relatively low risk. Current practice in close long-term follow-up is a thorough evaluation of new cardiopulmonary symptoms that should still be followed closely post-ERBT.

Study limitations

A primary limitation of this study is the sample size. As stated previously, this study was designed as a pilot study to determine the feasibility of using LGE-MRI to detect LA radiation damage for patients with EBRT history. We are currently planning the collection of more patient data post-EBRT to establish a better understanding of the precise relationship between LGE and EBRT dose. We also intend to differentiate other risk factors, such as age, gender, previous cardiac history, type of cancer, and concurrent chemotherapy. Furthermore, a pre-EBRT and/or pre-chemotherapy LGE-MRI acquisition for each patient under investigation should provide better information in establishing baseline. Regarding our image registration methodology, we used CT-MRI rigid image registration, which may be limited in ability to account for changes associated with long elapsed time between the 2 imaging modalities. To better address uncertainties that arise from positioning, motion, body shape change, and subjectivities, we plan to investigate deformable image registration for future studies. Other technical aspects, such as the spatial resolution in our CT dose mapping process was also limited. Depending on CT field of view settings, the pixel sizes from the seven patients studied ranged from 0.93 mm to 1.27 mm. With 2.5 mm slice thickness, the range of the voxel sizes of CT were 2.16-4.03 mm^3. These voxel size values are the smallest unit that can be accounted for in the TPS for dose calculation. As these values varied by patients according to their CT acquisition parameters, a standard protocol should be applied in the future for all of the patients under study. Finally, a histological/MRI correlation would add credibility by determining the specific tissue changes following EBRT-related injury, and will be the subject of further study.

Conclusions

In conclusion, it was demonstrated in this study that LGE-MRI can be used in detecting EBRT-induced myocardial tissue injury and the EBRT dose relationship with the left atrium tissue injury can be established. These findings may have important implications for survivors of thoracic neoplasms including lymphoma, esophageal, breast, and lung cancers. Imaging myocardial injury secondary to EBRT using MRI may be a useful

modality for following cardiac toxicity from EBRT, and in helping identify individuals who are more susceptible to EBRT damage. LGE-MRI may provide essential information to identify early screening strategies for affected cancer survivors after EBRT treatment. Further research is needed in LGE-MRI before this technique is applicable to routine clinical practice. Radiation-induced cardiac injury results in significant morbidity and mortality.[30] In 1 recent study of more than 40,000 esophagus patients, on multivariate analysis, radiation therapy was predictive of death from heart disease (hazard ratio, 1.46; $P < .05$) compared with patients that did not receive radiation therapy.[46] An early response indicator such as LGE-MRI may permit us to intervene in patients that receive a significant cardiac dose such as certain lung, esophagus, breast, and lymphoma patients. It is plausible that lifestyle interventions and medical therapy could help ameliorate the radiation therapy–induced damage.

References

1. Cuzick J, Stewart H, Rutqvist L, et al. Cause-specific mortality in long-term survivors of breast cancer who participated in trials of radiotherapy. *J Clin Oncol*. 1994;12:447-453.
2. Evans SB, Panigrahi B, Northrup V, et al. Analysis of coronary artery dosimetry in the 3-dimensional era: Implications for organ- at-risk segmentation and dose tolerances in left-sided tangential breast radiation. *Pract Radiat Oncol*. 2013;3:e55-e60.
3. Martel MK, Sahijdak WM, Ten Haken RK, Kessler ML, Turrisi AT. Fraction size and dose parameters related to the incidence of pericardial effusions. *Int J Radiat Oncol Biol Phys*. 1998; 40:155-161.
4. Mukherjee S, Aston D, Minett M, Brewster AE, Crosby TD. The significance of cardiac doses received during chemoradiation of oesophageal and gastro-oesophageal junctional cancers. *Clin Oncol (R Coll Radiol)*. 2003;15:115-120.
5. Wei X, Liu HH, Tucker SL, et al. Risk factors for pericardial effusion in inoperable esophageal cancer patients treated with definitive chemoradiation therapy. *Int J Radiat Oncol Biol Phys*. 2008;70:707-714.
6. Boivin JF, Hutchison GB, Lubin JH, Mauch P. Coronary artery disease mortality in patients treated for Hodgkin's disease. *Cancer*. 1992;69:1241-1247.
7. Hancock SL, Donaldson SS, Hoppe RT. Cardiac disease following treatment of Hodgkin's disease in children and adolescents. *J Clin Oncol*. 1993;11:1208-1215.
8. Hancock SL, Tucker MA, Hoppe RT. Factors affecting late mortality from heart disease after treatment of Hodgkin's disease. *JAMA*. 1993;270:1949-1955.
9. Aleman BM, van den Belt-Dusebout AW, De Bruin ML, et al. Late cardiotoxicity after treatment for Hodgkin lymphoma. *Blood*. 2007; 109:1878-1886.
10. Swerdlow AJ, Higgins CD, Smith P, et al. Myocardial infarction mortality risk after treatment for Hodgkin disease: A collaborative British cohort study. *J Natl Cancer Inst*. 2007;99: 206-214.
11. Cella L, Liuzzi R, Conson M, D'Avino V, Salvatore M, Pacelli R. Multivariate normal tissue complication probability modeling of heart valve dysfunction in Hodgkin lymphoma survivors. *Int J Radiat Oncol Biol Phys*. 2013;87:304-310.
12. Lee MS, Finch W, Mahmud E. Cardiovascular complications of radiotherapy. *Am J Cardiol*. 2013;112:1688-1696.
13. Gagliardi G, Constine LS, Moiseenko V, et al. Radiation dose-volume effects in the heart. *Int J Radiat Oncol Biol Phys*. 2010; 76(3 Suppl):S77-S85.
14. Gagliardi G, Lax I, Ottolenghi A, Rutqvist LE. Long-term cardiac mortality after radiotherapy of breast cancer—Application of the relative seriality model. *Br J Radiol*. 1996;69:839-846.
15. Das SK, Baydush AH, Zhou S, et al. Predicting radiotherapy-induced cardiac perfusion defects. *Med Phys*. 2005;32:19-27.
16. Lancellotti P, Nkomo VT, Badano LP, et al. Expert consensus for multi-modality imaging evaluation of cardiovascular complications of radiotherapy in adults: A report from the European Association of Cardiovascular Imaging and the American Society of Echocardiography. *Eur Heart J Cardiovasc Imaging*. 2013;14:721-740.
17. Mewton N, Liu CY, Croisille P, Bluemke D, Lima JA. Assessment of myocardial fibrosis with cardiovascular magnetic resonance. *J Am Coll Cardiol*. 2011;57:891-903.
18. Kwong RY, Chan AK, Brown KA, et al. Impact of unrecognized myocardial scar detected by cardiac magnetic resonance imaging on event-free survival in patients presenting with signs or symptoms of coronary artery disease. *Circulation*. 2006;113:2733-2743.
19. Assomull RG, Prasad SK, Lyne J, et al. Cardiovascular magnetic resonance, fibrosis, and prognosis in dilated cardiomyopathy. *J Am Coll Cardiol*. 2006;48:1977-1985.
20. Wu KC, Weiss RG, Thiemann DR, et al. Late gadolinium enhancement by cardiovascular magnetic resonance heralds an adverse prognosis in nonischemic cardiomyopathy. *J Am Coll Cardiol*. 2008;51:2414-2421.
21. Austin BA, Tang WH, Rodriguez ER, et al. Delayed hyper-enhancement magnetic resonance imaging provides incremental diagnostic and prognostic utility in suspected cardiac amyloidosis. *JACC Cardiovasc Imaging*. 2009;2:1369-1377.
22. O'Hanlon R, Grasso A, Roughton M, et al. Prognostic significance of myocardial fibrosis in hypertrophic cardiomyopathy. *J Am Coll Cardiol*. 2010;56:867-874.
23. Fallah-Rad N, Lytwyn M, Fang T, Kirkpatrick I, Jassal DS. Delayed contrast enhancement cardiac magnetic resonance imaging in trastuzumab induced cardiomyopathy. *J Cardiovasc Magn Reson*. 2008; 10:5.
24. McGann CJ, Kholmovski EG, Oakes RS, et al. New magnetic resonance imaging-based method for defining the extent of left atrial wall injury after the ablation of atrial fibrillation. *J Am Coll Cardiol*. 2008;52:1263-1271.
25. Oakes RS, Badger TJ, Kholmovski EG, et al. Detection and quantification of left atrial structural remodeling with delayed-enhancement magnetic resonance imaging in patients with atrial fibrillation. *Circulation*. 2009;119:1758-1767.
26. Maes F, Collignon A, Vandermeulen D, Marchal G, Suetens P. Multimodality image registration by maximization of mutual information. *IEEE Trans Med Imaging*. 1997;16:187-198.
27. Wells WM, Viola P, Atsumi H, Nakajima S, Kikinis R. Multi-modal volume registration by maximization of mutual information. *Med Image Anal*. 1996;1:35-51.
28. Eriksson F, Gagliardi G, Liedberg A, et al. Long-term cardiac mortality following radiation therapy for Hodgkin's disease: analysis with the relative seriality model. *Radiother Oncol*. 2000;55: 153-162.
29. Darby SC, Ewertz M, McGale P, et al. Risk of ischemic heart disease in women after radiotherapy for breast cancer. *N Engl J Med*. 2013;368:987-998.
30. Lyman JT. Complication probability as assessed from dose-volume histograms. *Radiat Res Suppl*. 1985;8:S13-S19.
31. Burman C, Kutcher GJ, Emami B, Goitein M. Fitting of normal tissue tolerance data to an analytic function. *Int J Radiat Oncol Biol Phys*. 1991;21:123-135.

32. Marks LB, Yorke ED, Jackson A, et al. Use of normal tissue complication probability models in the clinic. *Int J Radiat Oncol Biol Phys*. 2010;76(3 Suppl):S10-S19.
33. Deasy JO, Blanco AI, Clark VH. CERR: A computational environment for radiotherapy research. *Med Phys*. 2003;30:979-985.
34. Stewart JR, Fajardo LF. Dose response in human and experimental radiation-induced heart disease. Application of the nominal standard dose (NSD) concept. *Radiology*. 1971;99:403-408.
35. Carmel RJ, Kaplan HS. Mantle irradiation in Hodgkin's disease. An analysis of technique, tumor eradication, and complications. *Cancer*. 1976;37:2813-2825.
36. Cosset JM, Henry-Amar M, Pellae-Cosset B, et al. Pericarditis and myocardial infarctions after Hodgkin's disease therapy. *Int J Radiat Oncol Biol Phys*. 1991;21:447-449.
37. Stewart JR, Fajardo LF, Gillette SM, Constine LS. Radiation injury to the heart. *Int J Radiat Oncol Biol Phys*. 1995;31:1205-1211.
38. Adams MJ, Hardenbergh PH, Constine LS, Lipshultz SE. Radiation-associated cardiovascular disease. *Crit Rev Oncol Hematol*. 2003; 45:55-75.
39. Jaworski C, Mariani JA, Wheeler G, Kaye DM. Cardiac complications of thoracic irradiation. *J Am Coll Cardiol*. 2013;61:2319-2328.
40. Groarke JD, Nguyen PL, Nohria A, Ferrari R, Cheng S, Moslehi J. Cardiovascular complications of radiation therapy for thoracic malignancies: The role for non-invasive imaging for detection of cardiovascular disease. *Eur Heart J*. 2014;35:612-623.
41. Vordermark D, Seufert I, Schwab F, et al. 3-D reconstruction of anterior mantle-field techniques in Hodgkin's disease survivors: Doses to cardiac structures. *Radiat Oncol*. 2006;1:10.
42. Campbell BA, Hornby C, Cunninghame J, et al. Minimising critical organ irradiation in limited stage Hodgkin lymphoma: A dosimetric study of the benefit of involved node radiotherapy. *Ann Oncol*. 2012;23:1259-1266.
43. Koh ES, Tran TH, Heydarian M, et al. A comparison of mantle versus involved-field radiotherapy for Hodgkin's lymphoma: Reduction in normal tissue dose and second cancer risk. *Radiat Oncol*. 2007;2:13.
44. Joy S, Starkschall G, Kry S, Salehpour M, White RA, Lin SH, et al. Dosimetric effects of jaw tracking in step-and-shoot intensity-modulated radiation therapy. *J Appl Clin Med Phys*. 2012;13(2):3707.
45. Perry D, Morris A, Burgon N, McGann C, MacLoad R, Cates J. Automatic classification of scar tissue in late enhancement cardiac MRI for the assessment of left-atrial wall injury after radio frequency ablation. *Proc SPIE*. 2012;8315, 83151D-83151D9.
46. Frandsen J, Boothe D, Gaffney DK, Wilson BD, Lloyd S. Increased risk of death due to heart disease after radiotherapy for esophageal cancer. *J Gastrointest Oncol*. 2015;6:516-523.